Am J Transl Res 2023;15(10):6015-6025
www.ajtr.org /ISSN:1943-8141/AJTR0150571

Original Article

Diagnosis of kidney insufficiency by using the pressure waveforms of wrist-type sphygmomanometers: toward a convenient point-of-care device

Yu-Cheng Kuo[1,2], Chung-Yi Cheng[3,4,5], Lung-Ching Chen[6,7], Bashir Lawal[8], Po-Jen Shih[9], Hsu-Shan Huang[8,10,11]

[1]Department of Pharmacology, School of Medicine, College of Medicine, Taipei Medical University, Taipei 11031, Taiwan; [2]School of Post-Baccalaureate Chinese Medicine, College of Chinese Medicine, China Medical University, Taichung 40604, Taiwan; [3]Division of Nephrology, Department of Internal Medicine, School of Medicine, College of Medicine, Taipei Medical University, Taipei 11031, Taiwan; [4]Division of Nephrology, Department of Internal Medicine, Wan Fang Hospital, Taipei Medical University, Taipei 11031, Taiwan; [5]Research Center of Urology and Kidney, School of Medicine, College of Medicine, Taipei Medical University, Taipei 11031, Taiwan; [6]Division of Cardiology, Department of Internal Medicine, Shin Kong Wu Ho-Su Memorial Hospital, Taipei 11101, Taiwan; [7]School of Medicine, Fu Jen Catholic University, New Taipei 24205, Taiwan; [8]Graduate Institute for Cancer Biology and Drug Discovery, College of Medical Science and Technology, Taipei Medical University, Taipei 11031, Taiwan; [9]Department of Biomedical Engineering, National Taiwan University, Taipei 10617, Taiwan; [10]Graduate Institute of Medical Sciences, National Defense Medical Centre, Taipei 114, Taiwan; [11]Ph.D. Program in Biotechnology Research and Development, College of Pharmacy, Taipei Medical University, Taipei 11031, Taiwan

Received April 5, 2023; Accepted September 26, 2023; Epub October 15, 2023; Published October 30, 2023

Abstract: Objectives: Digital sphygmomanometers have been used for more than 40 years in Western medicine for accurately measuring systolic and diastolic blood pressures, which are vital signs observed for the diagnosis of different diseases. Similarly, traditional Chinese medicine (TCM) has been using wrist pulse diagnosis for thousands of years. Some studies have combined digital wrist pulse signals and the diagnosis method of TCM to quantify pulse waves and identify diseases. However, the effectiveness of this approach is limited because of scattered methods and complex pathological features. Moreover, the literature on TCM does not provide quantitative data or objective indicators. Methods: In this prospective study, we developed a diagnostic system that contains a modified sphygmomanometer. In addition, we designed a procedure for analyzing pulse waves with 156 features of harmonic modes and a decision tree method for diagnosing kidney insufficiency. Results: In the decision tree method, at least three features of harmonic modes can achieve an accuracy of 0.86, a specificity of 0.91, and a Cohen's kappa coefficient of 0.72. By comparison, the random forest method can achieve an accuracy of 0.99, a specificity of 0.99, and a Cohen's kappa coefficient of 0.94 within 200 trees. The results of this study indicated that even in patients with kidney insufficiency and complex etiology, common features can be distinguished by identifying changes in pulse waveforms. Conclusion: By using the modified sphygmomanometer to measure blood pressure, people can monitor their health status and take care of it in advance by simply measuring their blood pressure.

Keywords: Wrist-type sphygmomanometer, pulse diagnosis, harmonic modes, kidney insufficiency features, decision trees

Introduction

Digital sphygmomanometers are extensively used in medical institutions and homes, and more than 31 million new products are introduced to the market every year. Although these devices provide accurate measurements of systolic and diastolic blood pressures, the entire pressure waveforms measured by them do not provide physiological or pathological information. Similar to the use of wrist sphygmomanometers, wrist pulses have been used in traditional Chinese medicine (TCM) to diagnose and treat diseases since ancient times [1]. But in TCM, pulsations are felt by applying pressure with fingers at three locations on the wrists.

Pulse diagnosis depends on the subjective judgment of physicians and thus might be

Table 1. Baseline characteristics of the participants

	Kidney insufficient group (n = 200)		Normal group (n = 200)	
	Mean	SE	Mean	SE
Age (years old)	68.08	11.34	51.63	15.75
Male proportion	0.52	-	0.45	-
Heart rate	70.96	12.3	75.41	10.55
SBP (mmHg)	155.71	35.30	126.01	24.72
DBP (mmHg)	70.75	16.82	69.57	13.86
eGFR (mL/min/1.73 m^2)	5.27	0.38	-	-
BUN (mg/dL)	78.53	3.38	-	-
Creatinine (mg/dL)	10.39	0.45	-	-

Note: SBP, systolic blood pressure; DBP, diastolic blood pressure; eGFR, estimated glomerular filtration rate; BUN, blood urea nitrogen.

inconsistent. Such inconsistency has hindered the development of TCM techniques [2]. On the other hand, the miniaturization and enhanced sensitivity of electronic sensors have promoted the extensive development of diagnostic equipment that utilizes electronic pulses [2]. In addition, many pulse measurement equipment and platforms have been developed to collect pulse data for the diagnosis of four major categories of diseases [2]: (1) cardiovascular diseases [3]; (2) diabetes [4, 5], arteriosclerosis [6], and renal disease [7]; (3) arterial elasticity [8] and endothelial function-related diseases; and (4) other diseases, such as fatty liver [9], cholecystitis, nephrotic syndrome, pancreatitis, appendicitis, acute appendicitis, duodenal bulb ulcers, and three states of pregnancy [10]. However, the diagnosis of complex symptoms by using simple pulses is still challenging.

Kidney failure is a chronic condition in which one or both kidneys lose function. The causes of kidney failure are complex and include diabetes, high blood pressure, and acute kidney injuries; common treatment approaches are dialysis and transplant [11]. Chronic kidney disease (CKD) is characterized by abnormalities in kidney structure or function that persist for more than 3 months [12]. After the diagnosis of CKD, the glomerular filtration rate (GFR) should be determined, and the estimated GFR (eGFR) should be regularly assessed on the basis of various filtration markers [13]. According to the Annual Report of Kidney Disease in Taiwan (2021), the prevalence of patients with kidney disease in Taiwan who were receiving dialysis was 3.77%, which is severe, and the value is higher than the percentage of adults with low eGFR in the United States (i.e., 3.68%; USRDS, 2020). As per a report on the National Health Insurance (NHI) of Taiwan (2015-2019), since 2019, kidney dialysis has been the most expensive procedure covered by the NHI. This report revealed that 19.1%-19.7% of Taiwanese patients who received dialysis had not sought any medical attention before, and these patients with notable symptoms were observed after the disruption of renal function. On the other hand, preliminary research has revealed that TCM techniques can be effective in the diagnosis of kidney disease [7].

In pulse diagnosis, four types of signal preprocessing methods are employed for extracting pulse features [2]: transform-based methods, nonlinear methods, curve fitting-based methods, and measure-based methods. Among these methods, transform-based methods are the simplest. The fast Fourier transform (FFT) method is a transform-based signal preprocessing method that reveals frequency spectrum peaks and their corresponding amplitudes. However, the FFT method does not account for time variations, especially those in the local features of the pulse waveform in the time domain. Furthermore, in harmonic modal analysis, the first harmonic indicates a risk for nonfatal major adverse cardiovascular events [5], and a high fourth harmonic with a low third harmonic indicates a risk for diabetic retinopathy [4, 14] and other diseases [15, 16]. Therefore, in the present study, we used harmonic modal analysis, extracted the single waveform of each cycle, and applied an FFT to each waveform to obtain individual harmonic modes. To promote the use of TCM, we developed a pulse diagnosis measurement system based on the conventional wrist-type sphygmomanometer. We expect that a convenient point-of-care sphygmomanometer might be effective in the diagnosis of kidney insufficiency and facilitate timely medical attention.

Materials and methods

Study participants

A total of 400 participants were randomly recruited from the hemodialysis department of Taipei Municipal Wanfang Hospital, Taiwan. The cohort included 200 healthy participants and 200 patients undergoing hemodialysis treatment (**Table 1**). The participants were aged

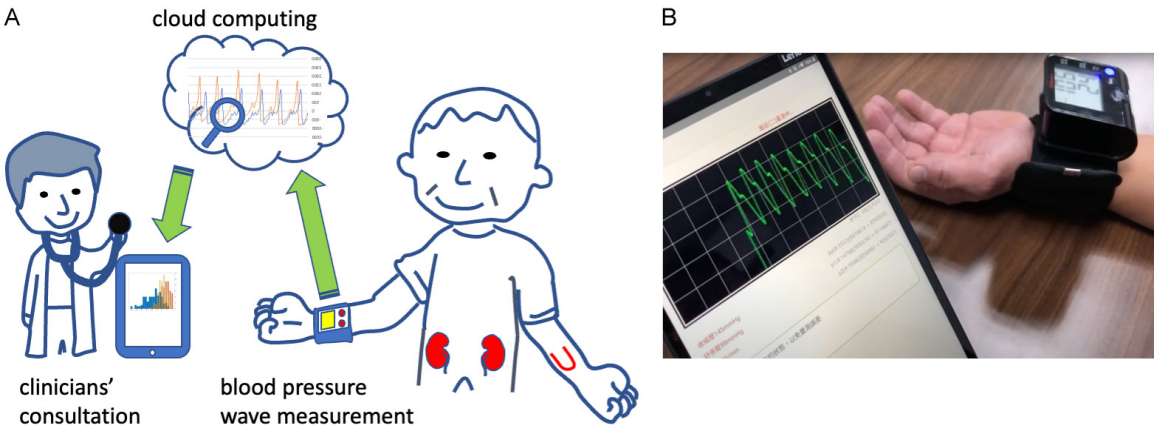

Figure 1. Potential convenient point-of-care devices for the proposed sphygmomanometer system: (A) Schematic illustrating self-measurement by a patient and diagnosis by a clinician; (B) Photograph of the proposed system, which comprises a wrist sphygmomanometer with an air-filled belt that is connected wirelessly to an electronic tablet.

between 20 and 90 years. The patients with kidney failure had GFRs of less than 60 mL/min, as determined by a professional nephrologist. Patients with severe arrhythmia, hypotension, and upper extremity tremors were excluded. This study was conducted under the ethical standards outlined in the Helsinki Declaration and through a retrospective research protocol approved by the Ethical Review Board of Taipei Medical University, Taiwan (IRB No. N202108016). The medical history and physical examination reports of the patients were compiled to determine their demographic data and clinical variables.

Experimental design

The participants were divided into two groups: one group contained 200 patients who had undergone hemodialysis treatment, and the other group contained 200 healthy participants. The blood pressure of the participants in both groups was measured in 5 minute sessions, in which the systolic blood pressure (SBP), diastolic blood pressure (DBP), and heart rates were obtained. The blood pressure waves of the participants were measured using a modified sphygmomanometer (HL158HA, Meridian Medicine blood pressure monitor, Modest Benefits Taiwan E Chain Co., Taiwan), and the signals were uploaded to a cloud computing platform, where the data were analyzed. The results were sent to electronic tablets to aid clinical consultation, as illustrated in **Figure 1**. We hypothesized that radial pulse waves contain physiological features of the kidney. The harmonic analysis of these waves revealed changes that indicated kidney failures. Therefore, we compared these changes among the different harmonic modes and applied decision trees to develop a diagnosis model.

Measurement of radial pulse waves

Blood circulation in the wrist artery involves a complex three-dimensional fluid-structure interaction between the blood in the artery and the arterial wall [17, 18]. TCM physicians detect pulse signals by adjusting boundary conditions such as pressures and positions on the surface of the wrist [19]. They use three fingers to feel the pressure waves emitted radially from the arterial wall, and they vary the application of force at adjacent positions (deep, middle, and superficial) of the wrist ("Cun", "Guan", and "Chi" [20]) to achieve different boundary conditions (**Figure 2A**). These boundary conditions affect the geometry of the local arterial wall and thus cause changes in the eigenfunctions and eigenfrequencies of this wall [21]. Thus, a certain range of frequencies may be amplified because of boundary effects [22, 23], and a physician can obtain a wide range of frequencies from the pulse signals by varying the positions of the fingers and the applied pressure.

To simulate the force applied by three fingers in this study, we varied the air pressure in the bowl belt of the modified sphygmomanometer and generated a pressure region around the artery (**Figure 2B**). This pressure was maintained for several seconds, and a pressure sensor was used to detect the radial pulse signals inside the air bowl belt (**Figure 2C**). The two pressures used in this study were P_1 (DBP) and

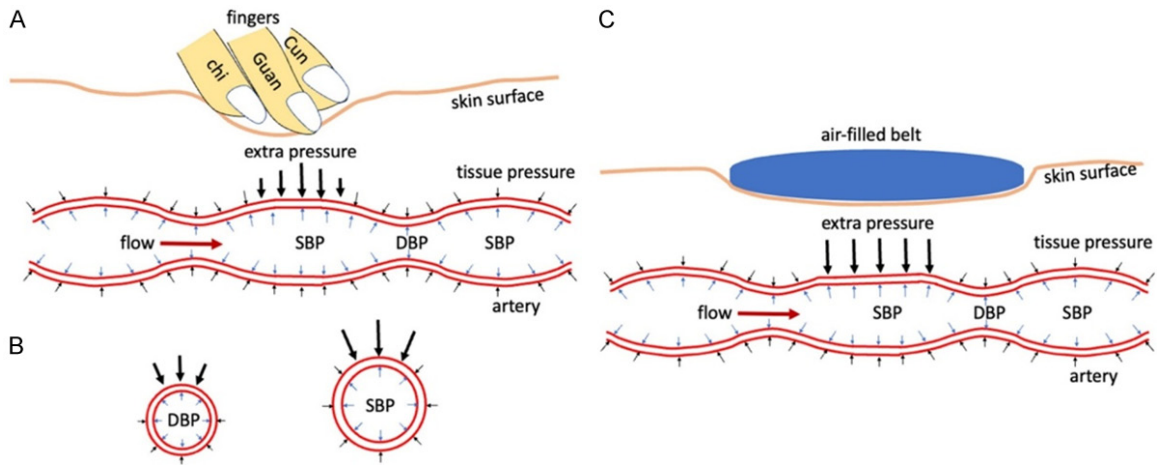

Figure 2. Schematic of conditions of the wrist when the physician observes pulse signals: (A) Longitudinal section depicting mechanical conditions, (B) Transversal section depicting the changing boundaries of the artery after pressure application, and (C) Longitudinal section depicting extra pressure conditions by air-filled belt.

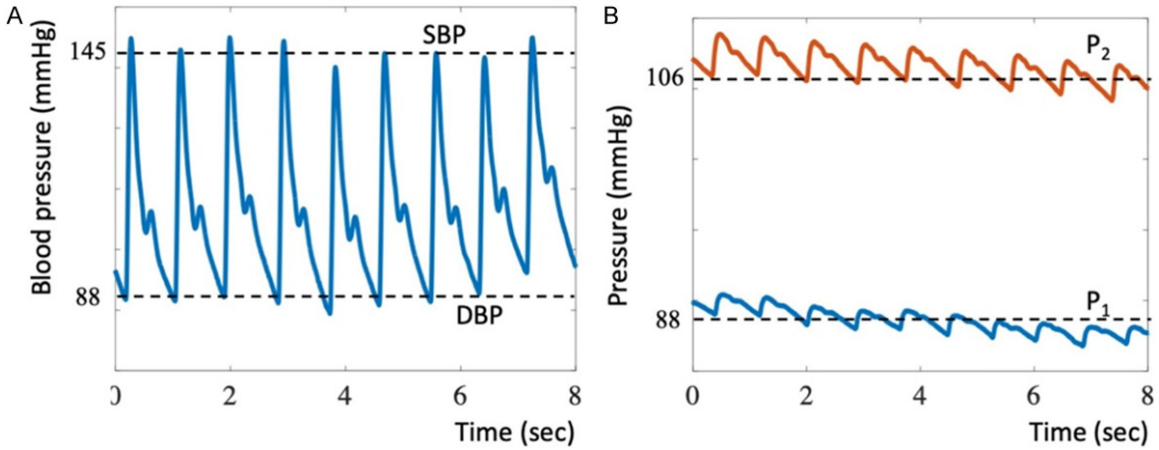

Figure 3. Blood pressure measurement with the modified sphygmomanometer: (A) The original pulse signal (with the SBP and DBP) of a participant; (B) Signals obtained at P_1 and P_2.

P_2 (mean arterial pressure; P_2 = (2/3) × DBP + (1/3) × SBP) (**Figure 3A**, **3B**). The DBP and SBP were measured before the two pressure tests (**Figure 3A**). The sampling rate was set at 500 s^{-1}, and the duration of each real measurement was 12 s.

Harmonic analysis of radial pulse waves

Eight pulse waveforms were recorded as raw data at the maintained pressures, as displayed in **Figure 4A**. The signals did not fluctuate regularly, as indicated by the fact that the signal envelopes were asymmetrical. We superimposed the recorded eight waveforms and set the lowest points as the starting points of the superposition (**Figure 4B**); the lowest points are indicated by green circles in **Figure 4A**. These waveforms had different durations and amplitudes. We selected the wavelength of the wave with the minimum duration as the cutoff wavelength for all waves. Subsequently, every wave with the same wavelength was duplicated to expand its duration for the fast Fourier transformation. After using an FFT, the amplitudes of the harmonic modes of these waves in the frequency domain were obtained. Because the duration of the waveform was small (Δt = 1.58 s), the discrete frequency spacing was relatively large (Δf = 0.632 Hz). So, the resolution in the frequency range (f = 0-12 Hz) was relatively low. The frequency amplitudes corresponding to each discrete frequency were different, as illustrated in **Figure 4C**. The order of the peaks

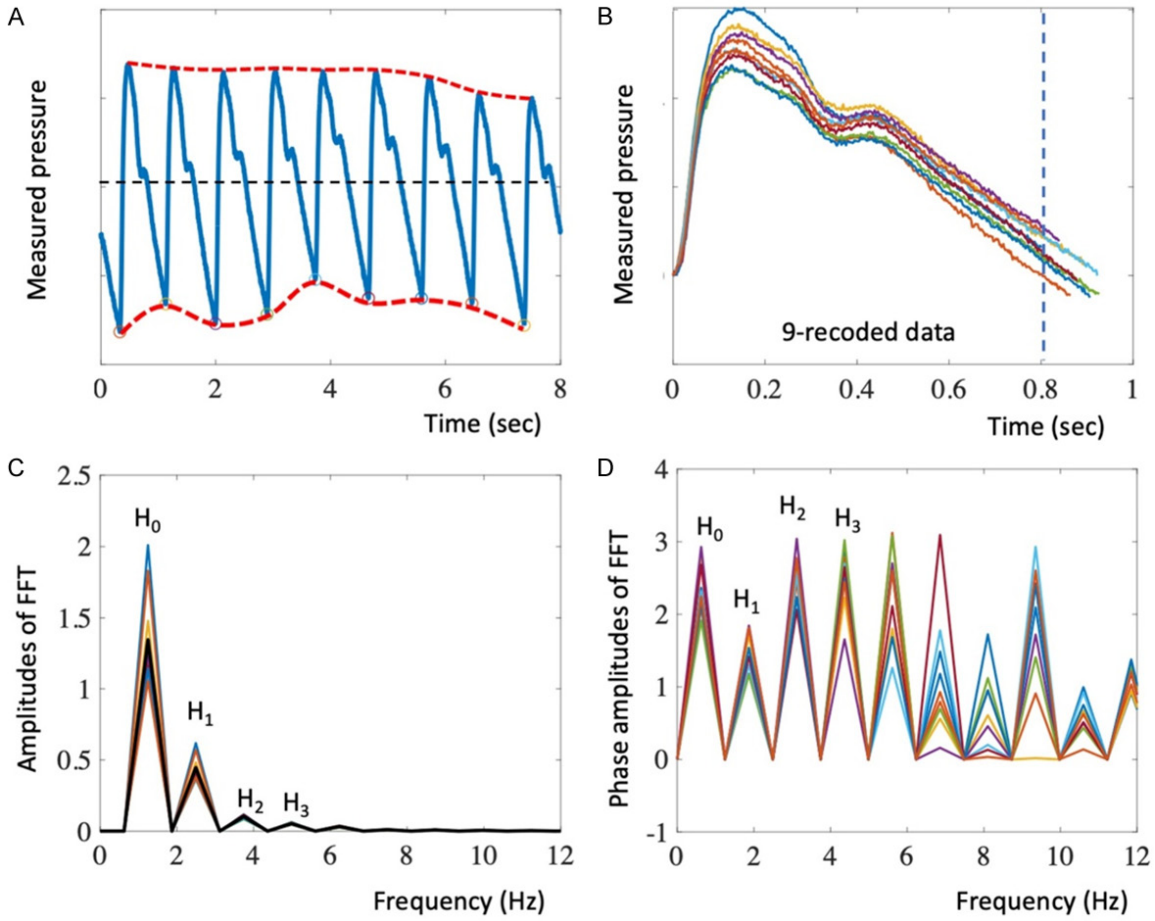

Figure 4. Measured radial pulse waves: (A) Raw pulse wave data; (B) Alignment of waveforms and their cutoff wavelengths; (C) Amplitudes of the FFT waveforms in the frequency domain; (D) Phases of the FFT waveforms.

was H_1, H_2, H_3, etc., as displayed in **Figure 4D**. Accordingly, the mean, standard deviation (STD), and coefficient of variation (CV) of these frequency amplitudes were obtained. In addition, the phase amplitudes and their associated CVs were obtained (**Figure 4D**).

Statistical analysis

The MATrix LABoratory (MATLAB, MathWorks, Inc., Natick, Massachusetts, USA) was used to analyze the data of all participants. To establish a modified prediction model, we applied random forest analysis and constructed prediction models for clinical applications by using Python codes (Python Software Foundation, Holland). We developed 200 trees for our prediction model. The minimum and maximum number of levels of trees in our model were 4 and 8, respectively. The accuracy, specificity, and Cohen's kappa coefficient of our models were 0.99, 0.99, and 0.94, respectively. The BP data of all participants were examined for normality by the Shapiro-Wilk (S-W) test and the results between grouping were compared. The *p*-value of the S-W method tested the normality of the data. The higher *p*-value did not reject the null hypothesis which conformed to the normal distribution, and the lower *p*-value represented rejecting the null hypothesis which does not conform to the normal distribution. Pearson correlation analysis was used to compare the amplitudes. We set the significance threshold at 0.05 for the two-sample t test for unpaired data. The *p* values were less than 0.001 for all harmonic modes except H_2 (P = 0.385), which indicated a significant correlation between the two groups. Data between treatment groups were analyzed and compared by Mean ± SD, and probability distributions. All the analysis results were fitted using the in-built "fitter" code of MATLAB.

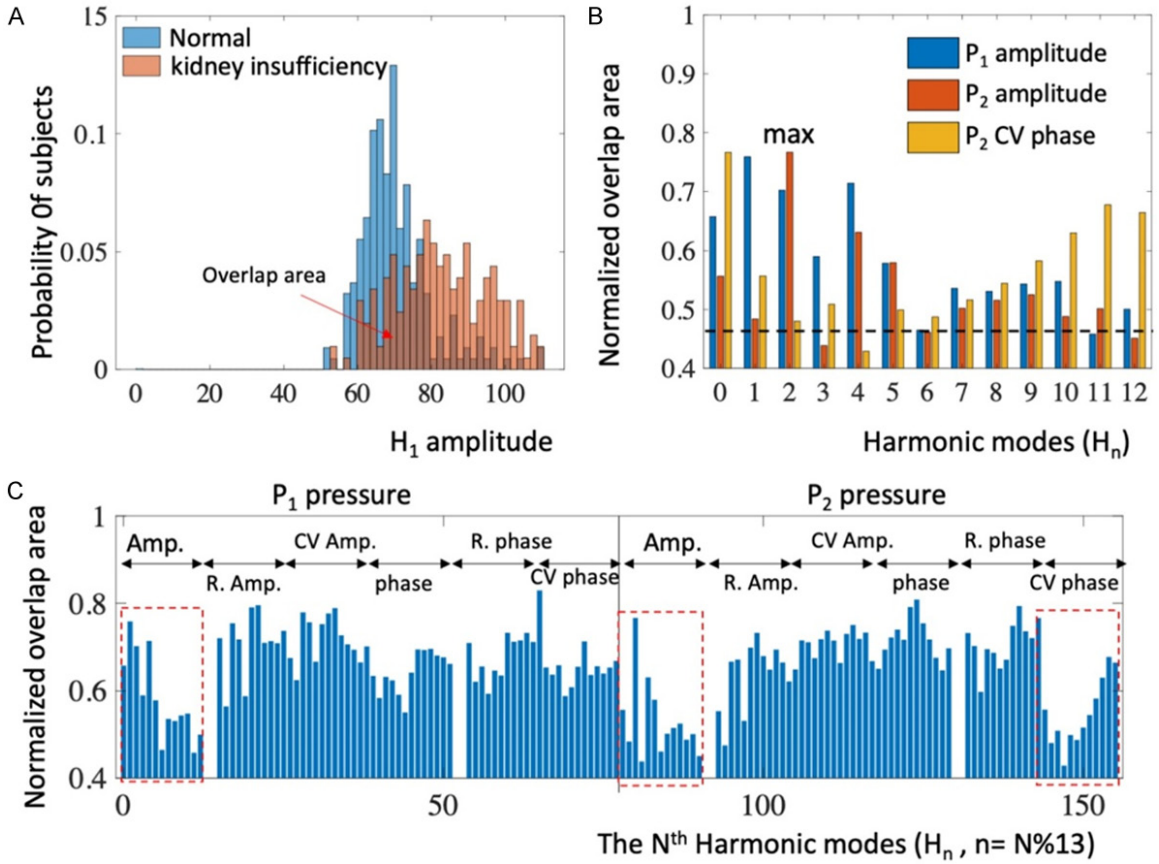

Figure 5. Statistical analysis of the normal group and the kidney insufficiency group: (A) Bar chart displaying the probability distributions of the H_1 amplitude at P_2 for the two groups. Here, H_1 is distinguishable between two groups. (B) Statistical values of the overlap area obtained from all parameters of the probability of statistical distributions under two pressure conditions for 12 clusters. The overlap areas were normalized in a range between 1 and 0. (C) Statistical values of the overlap area of the three clusters marked in (B). The harmonic modes (H_n, n = 0, 1, 2, 3,..., 12) and their related meridians are marked.

Results and discussion

Pressure waveforms of wrist-type sphygmomanometers for the diagnosis of kidney insufficiency

The SBP, DBP, amplitudes, ratios of amplitudes, CVs of amplitudes, phases, phase differences, and CVs of phases for the two groups were obtained at P_1 and P_2. For the first harmonic mode (H_1), the FFT amplitudes for the kidney insufficiency group ranged within 50-120, and those for the normal group ranged within 50-90 (**Figure 5A**). The probability distribution for the kidney insufficiency group was higher than that for the normal group, and we calculated the normalized overlap area between the two groups for the 156 parameters of the 12 clusters (**Figure 5B**). The overlapping areas of three clusters - amplitudes at P_1, amplitudes at P_2, and CVs of phases at P_2 - were relatively small. In addition, we compared these three clusters to determine the best parameters (**Figure 5C**). The smaller the overlapping area, the smaller the correlation between the two groups. Furthermore, the ratio results (**Table 2**) indicated that the amplitudes of all harmonic modes except H_0 and H_2 increased. Moreover, the STDs for all the harmonic modes except H_0 increased. We set the significance threshold at 0.05 for the two-sample t test for unpaired data. The *p* values were less than 0.001 for all harmonic modes except H_2 (P = 0.385), which indicated a significant correlation between the two groups.

Decision tree analysis

We determined the minimum number of possible parameters required to distinguish between patients with kidney insufficiency and normal participants. The two most important parame-

Table 2. Harmonic amplitudes at P_2 for the kidney insufficiency and normal groups

	Kidney insufficient group (n = 200)		Normal group (n = 200)		Ratio	
	Mean (M_k)	STD (S_k)	Mean (M_n)	STD (S_n)	M_k/M_n	S_k/S_n
H_0	4939.4	538.9	5411.4	567.86	0.91	0.95
H_1	84.59	15.15	69.94	10.80	1.21	1.40
H_2	35.27	8.20	35.48	6.43	0.99	1.28
H_3	19.81	4.70	15.02	3.64	1.32	1.29
H_4	11.16	3.00	9.61	2.02	1.16	1.49
H_5	8.74	2.14	7.20	1.66	1.21	1.29
H_6	6.16	2.11	4.25	1.32	1.45	1.60
H_7	4.13	1.60	2.80	0.86	1.48	1.86
H_8	3.04	1.36	2.04	0.72	1.49	1.90
H_9	2.28	1.13	1.39	0.59	1.64	1.91
H_{10}	1.70	0.92	0.92	0.45	1.84	2.05
H_{11}	1.27	0.73	0.64	0.34	1.98	2.12
H_{12}	0.98	0.58	0.45	0.26	2.21	2.27

ters with the smallest overlap area were selected (i.e., amplitude H_3 and the CV of phase H_4 at P_2). In the decision tree analysis performed in this study, two levels served as constraints, and the accuracy was 0.82, the specificity was 0.67, and the Cohen's kappa coefficient was 0.63 (indicating substantial agreement [24]). In addition, we added the third most important parameter, namely amplitude H_{12}, into the decision tree analysis and considered three levels. The accuracy increased to 0.86, the specificity increased to 0.913, and the Cohen's kappa coefficient increased to 0.72 (substantial agreement, **Figure 6A** and **6B**).

When only one cluster was considered [4, 19], the amplitudes at P_2 and the high-order modes (n > 10) were neglected to avoid low sensitivity, and the optimal sets with the selected parameters were (H_1, H_3, H_6) and (H_1, H_3, H_7) for three-level trees. The decision trees achieved accuracies of 0.82 and 0.82, specificities of 0.92 and 0.93, and Cohen's kappa coefficients of 0.63 and 0.64 (indicating substantial agreement), respectively (**Figure 6C** and **6D**). All the analysis results were fitted using the in-built "fitter" code of MATLAB.

Random forest analysis

To establish a modified prediction model, we applied random forest analysis and constructed prediction models for clinical applications by using Python codes (Python Software Foundation, Holland). We developed 200 trees for our prediction model. The minimum and maximum number of levels of trees in our model were 4 and 8, respectively. The accuracy, specificity, and Cohen's kappa coefficient of our models were 0.99, 0.99, and 0.94, respectively. Furthermore, we analyzed the importance of the parameters and determined the three most important parameters, namely amplitude H_3 at P_2, amplitude H_{12} at P_2, and phase variation H_4 at P_2 (**Figure 7**).

Discussion

On the basis of statistics and experimental results, classically dialectical studies on TCM have reported various identifying characteristics of pulse phases and corresponding herbal prescriptions [1]. Pulse diagnosis skills in TCM were transmitted orally or through clinical training from masters to apprentices. However, the results of the pulse diagnosis cannot be considered quantitative indicators. Therefore, studies have focused on identifying scientific indicators for diagnosis and have developed pulse diagnosis equipment, which, however, is expensive and currently in the laboratory development stage [25]. Furthermore, pulse signal identification is still challenging. Therefore, convenient and low-cost equipment, as well as home-care equipment, should be developed to implement TCM techniques for pulse diagnosis. The device developed in this study can be used to obtain accurate pulse wave information for pulse diagnosis based on the ancient wisdom of TCM. The modified sphygmomanometer should be initially used to examine the features of the pulse waveforms of patients with kidney

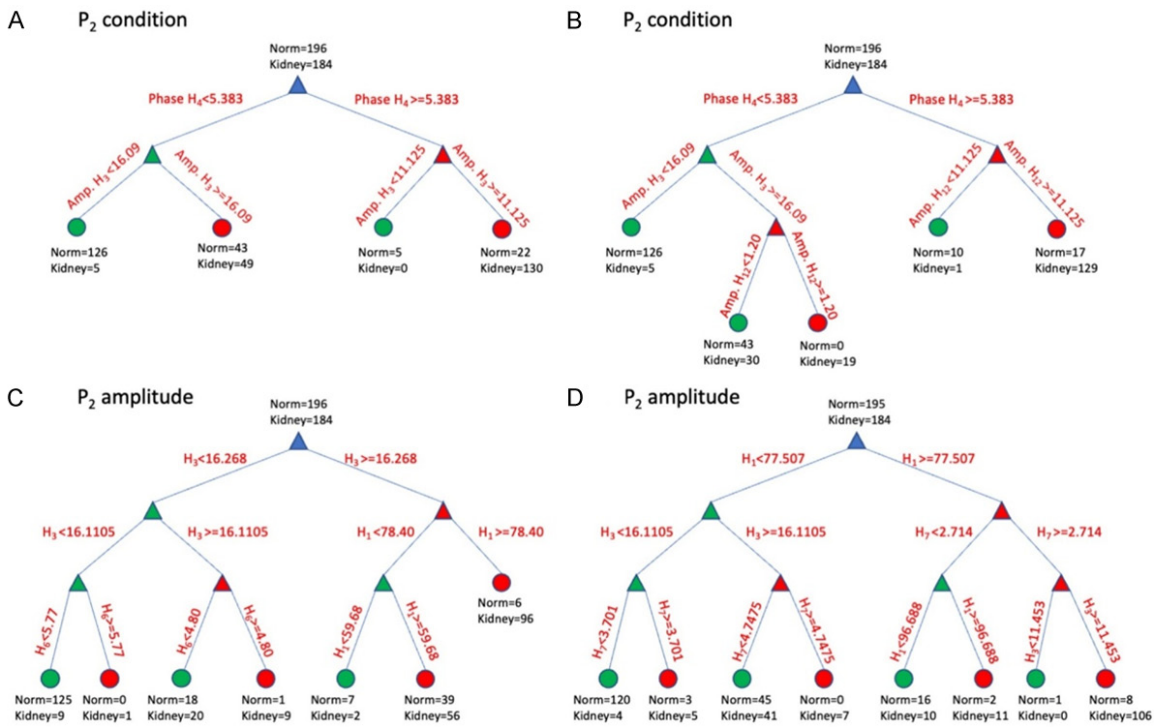

Figure 6. Simple decision trees for parameters at P_2. A. Amplitude H_3 and phase H_4; B. Amplitude H_3, amplitude H_{12}, and phase H_4; C. Amplitudes H_1, H_3, and H_6; D. Amplitudes H_1, H_3, and H_7.

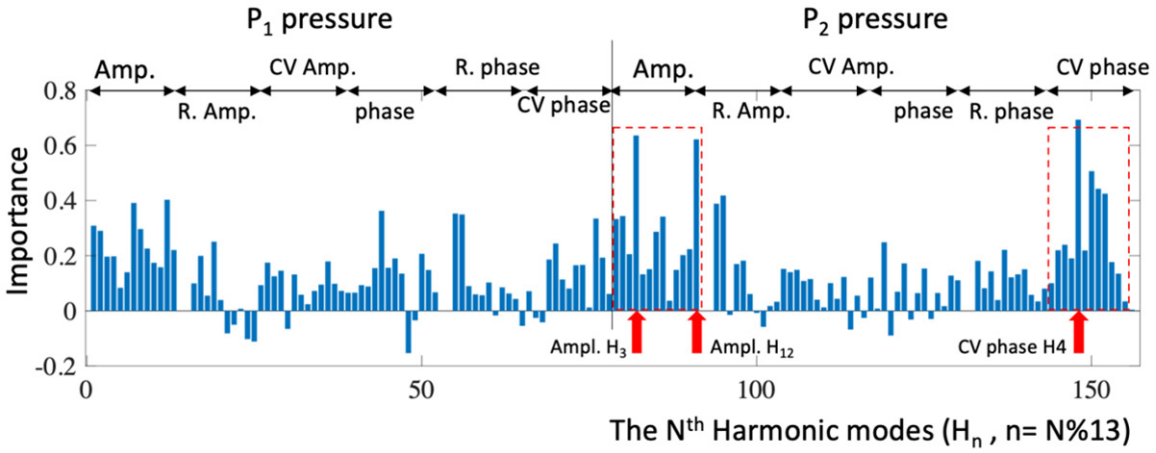

Figure 7. Importance of the major parameters of two selected clusters.

insufficiency. Once a large quantity of data is collected, predictive models can be subjected to statistical training for the prediction of certain diseases and the development of convenient point-of-care devices.

This study was inspired by previous investigations by our advisor [17, 26, 27], who demonstrated a correlation between acute hepatotoxicity and type 2 diabetes with different harmonic modes. In the present study, we used additional features and advanced techniques to explore the diagnosis of kidney disease. Furthermore, to improve pulse diagnosis equipment with three fingers [2], we adjusted the pressure in the air-filled chamber of a wrist belt and measured signals in the air chamber instead of using fingers to apply force at certain positions. In addition, we hypothesized that the overall signal detection around the wrist might include signals from the belt-covered area (i.e., signals from three positions, namely Cun, Guan,

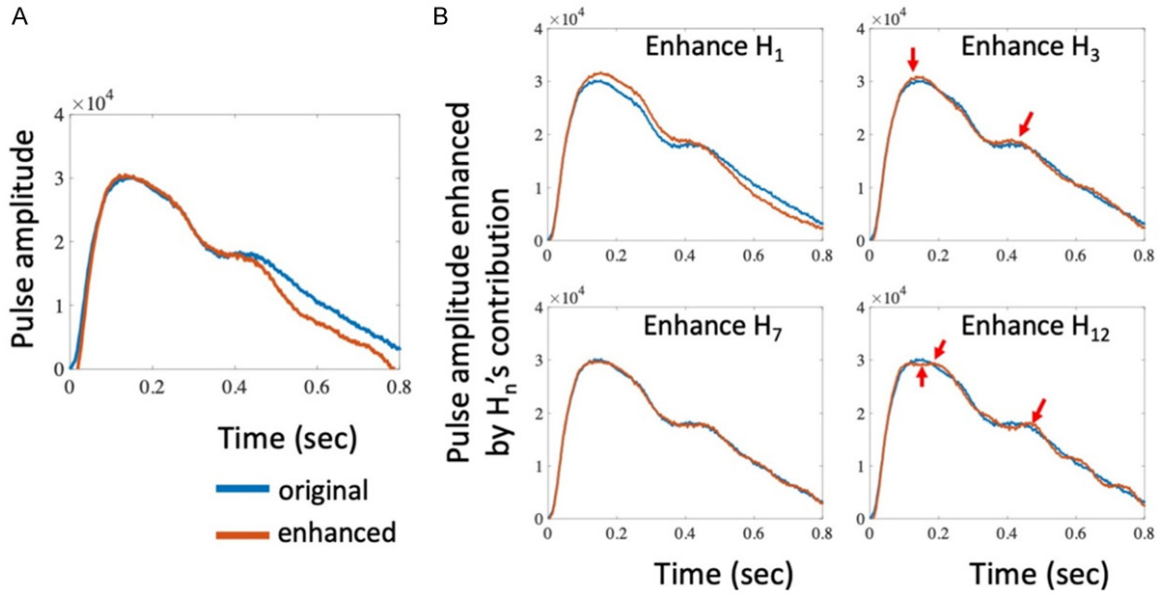

Figure 8. Modified waveform obtained through the simulation of the kidney insufficiency group and the comparison of this waveform with the original waveform. A. Harmonic modes enhanced and compared with the original waveform; B. Specific modes enhanced, such as only H_1, H_3, H_7, and H_{12}.

and Chi). Note that strong correlations at these positions were demonstrated by Li et al. [20].

In this study, we modified the progression of harmonic wave analysis. First, we reduced the frequency resolution spacing (Δf) to enhance the stability of amplitude and phase calculations. Second, in the waveform analysis, we selected the lowest points to align every waveform, selected the wavelength of the minimum-duration waveform as the cutoff wavelength, and expanded the wavelength by duplicating the single waveform before using an FFT. We did not scale the wavelength to normalize it and to prevent the shifting of the real frequency. The two modifications reduced computational complexity and promoted the stability of numerical solutions, thereby increasing the repeatability of the measurements. However, the proposed method has a few limitations. First, the cutoff wavelength causes discontinuities in the interface of the two duplicated waveforms, and the discontinuities induce an additional contribution to the frequency spectrum, but only for frequencies higher than 50 Hz. Second, although the proposed method reduces noise, it also decreases the frequency spacing resolution. Third, our method neglects the baseline wander (the asymmetry of the envelopes) in the pulse waveform that may reflect other diseases. For the baseline wander, see reference [19].

Our data suggested that the parameters corresponding to P_2 were more effective for identifying kidney insufficiency than those corresponding to P_1. In the decision tree analysis, we restricted the fit level number to the number of parameters, which helped prevent the overfitting caused by the presence of many thresholds and levels and enabled the achievement of customized results. Moreover, the three most important parameters were also shown in the random forest method, and the amplitude and the phase CV clusters at P_2 were also better than other clusters.

Pulse diagnosis in TCM relies heavily on identifying pressure differences by touching with fingers [28]. To visualize these differences, we obtained the waveforms for the normal participants (**Figure 4A**) and used them as base waveform to simulate changes in the waveforms for patients with kidney insufficiency. **Table 2** lists the ratios obtained by comparing the parameters of the kidney insufficiency and normal groups. We applied these ratios to adjust the amplitudes at modal frequencies and simulate the amplitudes for kidney insufficiency. By implementing an inverse FFT on harmonic modes, we obtained modified time-domain waveforms, as displayed in **Figure 8A**. The differences between the modified waveform and original waveform indicated differences

in blood pressure between the two groups. Moreover, we used the single mode to identify the key characteristics among the previously selected parameters (**Figure 8B**). The amplitude and wavelength of the waveform increased when H_1 was enhanced; the intensity of the waveform increased when H_3 was enhanced; the noise in the waveform increased when H_7 was enhanced; and the waveform contained wavelets when H_{12} was enhanced.

The dominant frequencies of healthy participants were in similar frequency ranges to those observed in previous relevant studies [19, 20, 29, 30], which indicated the accuracy of the method proposed in this study. However, this study is limited by its use of two pressure steps (P_1 and P_2), which are insufficient compared with the three pressure steps used in the pulse detection method in TCM. In particular, the light (Fu), moderate (Zhong), and heavy (Chen) forces applied at the three positions - Cun, Guan, and Chi - are night combinations. Despite this limitation, the modified device developed in this study is equipped with highly sensitive pressure sensors to enhance signals. The analysis results indicated the existence of frequency doubling, which suggests that the proposed method does not neglect key frequencies. Another limitation of this study is the amplitude values, which will be more comparable to real values once sufficient statistical data are obtained.

Conclusions

In this study, we developed a modified wrist-type sphygmomanometer to detect pressure waveforms for the diagnosis of diseases. A simple air-pressure wristband with a highly sensitive pressure sensor was applied as an alternative to the three-point, pulse-detecting technique implemented in other devices. Our data suggested that the use of sphygmomanometers for measuring blood pressure is convenient, accurate, and well-established in modern clinics and can be extended to TCM clinics to aid pulse diagnosis and care.

Acknowledgements

H.-S. Huang is funded by the National Science and Technology Council, Taiwan, grant number NSTC111-2314-B-038-017 and the Ministry of Science and Technology, Taiwan, grant number MOST111-2314-B-038-122.

Disclosure of conflict of interest

The authors declare that the research was conducted in the absence of any commercial or financial relationships that could be construed as a potential conflict of interest.

Address correspondence to: Dr. Po-Jen Shih, Department of Biomedical Engineering, National Taiwan University, Taipei 10617, Taiwan. E-mail: pshih@ntu.edu.tw; Dr. Hsu-Shan Huang, Graduate Institute for Cancer Biology and Drug Discovery, College of Medical Science and Technology, Taipei Medical University, Taipei 11031, Taiwan. Tel: +886-2-6638-2736 Ext. 1377, +886-0938-396023; E-mail: huanghs99@tmu.edu.tw; huanghs99@gmail.com

References

[1] Schmidt MWGA. Huangdi Neijing - Suwen, Lingshu and Nanjing. Berlin: Viademica-Verlag; 2007.

[2] Guo C, Jiang Z, He H, Liao Y and Zhang D. Wrist pulse signal acquisition and analysis for disease diagnosis: a review. Comput Biol Med 2022; 143: 105312.

[3] Guo R, Wang Y, Yan H, Yan J, Yuan F, Xu Z, Liu G and Xu W. Analysis and recognition of traditional Chinese medicine pulse based on the Hilbert-Huang transform and random forest in patients with coronary heart disease. Evid Based Complement Alternat Med 2015; 2015: 895749.

[4] Liao KM, Wang SH, Tsai LT, Chen YC, Wang TC and Wang GC. A non-invasive harmonic analysis to assess risk of retinopathy in type 2 diabetes mellitus. J Diabetes Complications 2022; 36: 108306.

[5] Chang CW, Liao KM, Chang YT, Wang SH, Chen YC and Wang GC. The effect of radial pulse spectrum on the risk of major adverse cardiovascular events in patients with type 2 diabetes. J Diabetes Complications 2019; 33: 160-164.

[6] Chang CW, Liao KM, Chang YT, Wang SH, Chen YC and Wang GC. The first harmonic of radial pulse as an early predictor of silent coronary artery disease and adverse cardiac events in type 2 diabetic patients. Cardiol Res Pract 2018; 2018: 5128626.

[7] Yudaningtyas E, Santjojo DH, Djuriatno W, Siradjuddin I and Hidayatullah MR. Identification of pulse frequency spectrum of chronic kidney disease patients measured at TCM points using FFT processing. 2017 15th International Conference on Quality in Research (QiR) - International Symposium on Electrical and Computer Engineering. 2017. pp. 169-172.

[8] Bae JH and Jeon YJ. Pulse sharpness as a quantitative index of vascular aging. Sci Rep 2021; 11: 19895.
[9] Nanyue W, Youhua Y, Dawei H, Bin X, Jia L, Tongda L, Liyuan X, Zengyu S, Yanping C and Jia W. Pulse diagnosis signals analysis of fatty liver disease and cirrhosis patients by using machine learning. ScientificWorldJournal 2015; 2015: 859192.
[10] Liao YT, Chen HY, Huang CM, Ho M, Lin JG, Chiu CC, Wang HS and Chen FJ. The pulse spectrum analysis at three stages of pregnancy. J Altern Complement Med 2012; 18: 382-386.
[11] Levey AS and Coresh J. Chronic kidney disease. Lancet 2012; 379: 165-180.
[12] Chen TK, Knicely DH and Grams ME. Chronic kidney disease diagnosis and management: a review. JAMA 2019; 322: 1294-1304.
[13] Levey AS, Becker C and Inker LA. Glomerular filtration rate and albuminuria for detection and staging of acute and chronic kidney disease in adults: a systematic review. JAMA 2015; 313: 837-846.
[14] Chang CW, Liao KM, Chang YT, Wang SH, Chen YC and Wang GC. Fourth harmonic of radial pulse wave predicts adverse cardiac events in asymptomatic patients with type 2 diabetes. J Diabetes Complications 2019; 33: 413-416.
[15] Kuo YC, Chiu TY, Jan MY, Bau JG, Li SP, Wang WK and Wang YY. Losing harmonic stability of arterial pulse in terminally ill patients. Blood Press Monit 2004; 9: 255-258.
[16] Hsu TL, Chao PT, Hsiu H, Wang WK, Li SP and Wang YY. Organ-specific ligation-induced changes in harmonic components of the pulse spectrum and regional vasoconstrictor selectivity in Wistar rats. Exp Physiol 2006; 91: 163-170.
[17] Wang YYL and Wang WK. A hemodynamics model to study the collective behavior of the ventricular-arterial system. J Appl Phys 2013; 113: 1015-726.
[18] Wang D, Vahala L and Hao ZL. Radial and longitudinal motion of the arterial wall: their relation to pulsatile pressure and flow in the artery. Phys Rev E 2018; 98: 032402-1-032402-8.
[19] Wang DM, Zhang D and Lu GM. A robust signal preprocessing framework for wrist pulse analysis. Biomed Signal Process Control 2016; 23: 62-75.
[20] Li N, Yu JR, Hu HQ, Mao XB, Zhao YP and Huang LQ. The correlation study of Cun, Guan and Chi position based on wrist pulse characteristics. IEEE Access 2021; 9: 28917-28929.
[21] Kreyszig H and Norminton EJ. Advanced Engineering Mathematics. Hoboken, N.J.: Wiley; 2011.
[22] Shih PJ, Wu SJ, Sung YH, Tung YT, Chang CY, Hatamie S and Dai ZX. Eye orbit effects on eyeball resonant frequencies and acoustic tonometer measurements. Sci Rep 2022; 12: 4883.
[23] Kumari R, Kumar P, Kumar N and Sandeep. Role of site effect for the evaluation of attenuation characteristics of P, S and coda waves in Kinnaur region, NW Himalaya. J Earth Sys Sci 2020; 129.
[24] Landis JR and Koch GG. The measurement of observer agreement for categorical data. Biometrics 1977; 33: 159-174.
[25] Bayoumy K, Gaber M, Elshafeey A, Mhaimeed O, Dineen EH, Marvel FA, Martin SS, Muse ED, Turakhia MP, Tarakji KG and Elshazly MB. Smart wearable devices in cardiovascular care: where we are and how to move forward. Nat Rev Cardiol 2021; 18: 581-599.
[26] Hsu TL, Chiang Y, Wang WK, Chao PT, Bao JG and Wang YY. Pulse analysis as a possible real-time biomarker complementary to SGPT and SGOT for monitoring acute hepatotoxicity. Toxicol Mech Methods 2003; 13: 181-186.
[27] Wang WK, Bau JG, Hsu TL and Wang YY. Influence of spleen meridian herbs on the harmonic spectrum of the arterial pulse. Am J Chin Med 2000; 28: 279-289.
[28] Yeh HY, Zhan X and Qi W. A comparison of ancient parasites as seen from archeological contexts and early medical texts in China. Int J Paleopathol 2019; 25: 30-38.
[29] Xue YA, Su Y, Zhan C, Xu XH, Gao ZR, Wu SQ, Zhang QC and Wu XP. Full-field wrist pulse signal acquisition and analysis by 3D digital image correlation. Optics Lasers Eng 2017; 98: 76-82.
[30] Peng B, Luo CH, Sinha N, Tai CC, Xie X and Xie H. Fourier series analysis for novel spatiotemporal pulse waves: normal, taut, and slippery pulse images. Evid Based Complement Alternat Med 2019; 2019: 5734018.